On Modelling Nitrogen Species as Pollutants: Thermochemical Influences

John Bugler[a], Kieran P. Somers[a], John M. Simmie[a], Felix Güthe[b], Henry J. Curran[a,*]

[a]Combustion Chemistry Centre, National University of Ireland, Galway H91 TK33, Ireland

[b]GE Power – GSTRB, Brown Boveri Strasse 7, 5401 Baden, Switzerland

ABSTRACT

In order to simulate emissions of nitrogen-containing compounds in practical combustion environments, it is necessary to have accurate values for their thermochemical parameters, as well as accurate kinetic values to describe the rates of their formation and decomposition. Significant disparity is observed in the literature for the former, and we therefore present herein high-accuracy *ab initio* gas-phase thermochemistry for 60 nitrogenous compounds, many of which are important in the formation and consumption chemistry of NO_x species. Several quantum-chemical composite methods (CBS-APNO, G3, and G4) were utilised in order to derive enthalpies of formation *via* the atomisation method. Entropies and heat capacities were calculated from traditional statistical thermodynamics, with oscillators treated as anharmonic based on ro-vibrational property analyses carried out at the B3LYP/cc-pVTZ level of theory. The use of quantum chemical methods, along with the treatments of anharmonicities and hindered rotors, ensures accurate enthalpy of formation, entropy, and heat capacity values across a temperature range of 298.15–3000 K. The implications of these results for atmospheric and combustion modelling are discussed.

TOC graphic

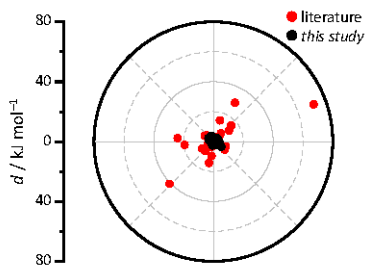

1. INTRODUCTION

With ever more stringent emissions regulations and growing environmental concerns, controlling emissions of nitrogen oxides (NO_x) from combustion and high-temperature industrial processes continues to be an active area of research. Combustor design and fuel flexibility can both aid in the quest to reduce these harmful emissions. However, making improvements in these areas needs to be carried out in an efficient and cost-effective way if timely progress is to be made. To this end, the use of chemical kinetic models has been invaluable, and in recent years there have been quite a few proposed mechanisms concerned with NO_x chemistry, and with interactions of nitrogen oxides with hydrocarbons.[1–18] However, as will be discussed, there can be significant disparity between published models in terms of the thermochemical properties of nitrogen-containing species therein. This is often coupled with further disparity in terms of kinetic rate parameters within the models. The two are likely linked and, as has been highlighted previously[19], erroneous kinetic and thermodynamic values within a chemical kinetic model can lead to a series of compensating errors, resulting in favourable agreement with a limited set of experimental validation targets. It seems, much like models describing hydrocarbon oxidation, the "many-model" problem[20–22] appears to also apply to descriptions of NO_x chemistry. If there is to be convergence towards a comprehensive description of NO_x chemistry, an accurate and, importantly, a consistent set of thermochemical data for important nitrogenous species is necessary. This study addresses this problem by providing a comprehensive database of theoretically-derived-experimentally-calibrated enthalpies, along with heat capacities, entropies, and Gibbs energies for the full panoply of nitrogen-containing species found in literature models for NO_x formation.

Methods used to derive thermochemical values, comparison with literature values, and their implications for atmospheric and combustion modelling will be discussed.

2. COMPUTATIONAL METHODS

Molecular geometry optimisations and ro-vibrational analyses have been determined for each species using the B3LYP functional[23] coupled with the cc-pVTZ basis set.[24] This functional used in conjunction with triple-ζ basis sets has been found to provide agreement with experimentally measured vibrational frequencies that requires little modification (i.e. scale factors close to unity).[25] Furthermore, the high-accuracy *ab initio* transition state theory master equation (AITSTME) approach of Klippenstein and co-workers utilises B3LYP/cc-pVTZ to calculate anharmonic zero-point energy corrections.[26] All density functional theory and composite method (vide infra) calculations have been performed using the Gaussian 09 software package.[27]

The influence of low-frequency torsional modes on the thermodynamic properties of interest has been considered *via* a 1-D hindered rotor approximation, and an explicit consideration of true vibrational anharmonicity is considered for all other degrees of freedom. For the treatment of torsional modes, relaxed potential energy surface (PES) scans were carried out also using the B3LYP functional with the cc-pVTZ basis set, with the molecular geometry and single-point energy of each structure determined during dihedral scans at 10 degree intervals. Rotational constants about the torsional centre-of-mass were computed as a function of dihedral angle using the Lamm module of the MultiWell program suite.[28] Both the potential energy and rotational constants were fitted to truncated Fourier series, and used as input to compute energy levels and hence the partition function of the mode.

For true vibrational modes, anharmonicity has been accounted for *via* the method of Barone[29], which allows the determination of the full matrix of anharmonicity constants (χ_{ij}) for each vibrational degree of freedom in a molecule. Together with the harmonic frequencies, the diagonal elements (χ_{ii}) of this matrix have been used to compute $0 \rightarrow 1$ fundamental frequencies. These fundamental frequencies are then used un-scaled, together with the anharmonicity constants (χ_{ii}), as input for the Thermo module of MultiWell. Comparing the resulting values with the more commonplace approach

of using empirically optimised frequency scale factors to correct partition functions for quantum chemical uncertainties in vibrational analysis shows relatively small differences. For example, nitromethane (CH_3NO_2) shows differences of approximately 0.1 kJ mol^{-1} in enthalpy of formation, and 0.3 and 0.8 J K^{-1} mol^{-1} in entropy and heat capacity, respectively, at 298.15 K, rising to 2.9 kJ mol^{-1}, and 3.2 and 2.0 J K^{-1} mol^{-1} at 2000 K. Though the differences are small, the latter approach cannot adequately account for the temperature-dependence of these properties when compared with a more explicit treatment of anharmonicity. Other corrections may influence the calculated thermodynamic properties of the investigated species (spin-orbit corrections, higher order correlation, etc.[30]), but here we choose to investigate the effect of anharmonicities. Further investigations are warranted to assess the influence of other factors, though these are likely to be minor.

In some instances, a failure is observed when computing 0→1 fundamental frequencies, manifested as the occurrence of negative values. Negative anharmonic frequencies are calculated for aminoxyl (H_2NO), cyanato (NCO), and nitrate (NO_3) radicals. In light of this, properties for these three species are presented based on the assumption that the vibrations behave as harmonic oscillators. However, due to the low number of atoms in these species, corrections for anharmonicities are expected to be quite small, with similarly-sized molecules exhibiting differences of approximately 1 kJ mol^{-1} and 1 J K^{-1} mol^{-1} in enthalpies of formation and entropies, respectively, at 2000 K. Hence, these failures do not undermine the validity of our updated database, particularly when we consider the relative improvement with respect to available models.

Where possible, 0 K enthalpies of formation have been adopted from a database of these values for nitrogen species obtained in the recent study by Simmie.[31] For several of the species investigated therein, enthalpies of formation were determined *via* the use of isodesmic reactions, ensuring "chemically accurate" uncertainty bounds. For species not present in the aforementioned study, the values of interest have been determined *via* the atomisation method using the average values

obtained from CBS-APNO, G3, and G4 compound methods.[32–34] This combination of methods has been found to yield results rivalling "chemical accuracy" (arbitrarily, ~4 kJ mol^{-1}, or 1 kcal mol^{-1}) when benchmarked against enthalpy of formation values in the Active Thermochemical Tables (ATcT).[35–37]

Anharmonic frequencies, hindered rotor corrections, 0 K enthalpies of formation (all calculated herein), and electronic energy levels (as tabulated in the Computational Chemistry Comparison and Benchmark DataBase, CCCBDB[38]) were used as input for the Thermo module of MultiWell for computation of the thermochemical values of interest as a function of temperature (298.15–3000 K). The resulting values were fitted to NASA polynomials[39] using the Fitdat utility in CHEMKIN-PRO.[40] These polynomials are available as Supporting Information. Table S1 in the Supporting Information also lists 298.15 K enthalpies of formation and entropies, alongside heat capacity values at selected temperatures in the range 300–1500 K, as is standard input/output format for the THERM software package.[41] These outputs should be compatible with most kinetic modelling software of widespread use in academia and industry.

3. RESULTS AND DISCUSSION

3.1. Comparison with literature values

Figure 1 (a) shows Tukey mean-difference, or Bland-Altman[31,42], plots of enthalpies of formation from the ATcT versus those presented here. Differences between the values are defined as: $d_i = (\mathrm{ATcT} - \bar{x}_i)$, with the mean difference, or *bias*, expressed as:

$$\bar{d} = \sum_{i}^{n} (\mathrm{ATcT} - \bar{x})/n = \sum_{i}^{n} (d_i)/n \qquad (1)$$

In Fig. 1 (a), a slight negative bias is observed (–0.4 kJ mol^{-1}), with 95% confidence intervals lying 3.8 kJ mol^{-1} about this measure of central tendency, assuming the differences are normally distributed. The confidence intervals are defined as ~1.96s_d, where s_d is the standard deviation in $\bar{d}$, given by[43]:

$$s_d = \sqrt{\frac{\sum\left(d_i - \bar{d}\right)^2}{(n-1)}} \quad (2)$$

Error bars in Fig. 1 are computed from: $t \times s_d/\sqrt{n}$

for the bias, and: $1.709 \times t \times s_d/\sqrt{n}$

for the limits of agreement, where t is Student's t-value at the 95% confidence, and n is the number of data points.

This level of agreement with what is the best available repository of enthalpies of formation, essentially calibrates the results calculated as part of this work, and allows for assessment of other literature values *via* direct comparisons. This approach is necessary as many species in literature models do not have corresponding values in the ATcT.

While the average values of the aforementioned composite methods resulted in adequate overall agreement with the ATcT, the formation enthalpy values of four of the studied species (CN, NCN, NO_2, and NO_3) were further refined with computations using the high-accuracy W3X-L method.[44] The use of this method comes at a significantly higher computational cost than that of the CBS and G*n* methods, but incorporates calculations which can provide accurate results for species which exhibit multireference character. The T_1 diagnostic of Lee and Taylor[45] is often used as a measure of tendency towards exhibiting this characteristic, with values over 0.02 being indicative of cases where single reference methods to describe the wavefunction may not be appropriate. Of the four species re-examined using W3X-L, NO_2 has the lowest T_1 value (~0.03) and does not appear to strongly exhibit multireference character. However, the other three cases have values in the 0.05–0.11 range, which is exceptionally high. Agreement between the formation enthalpy values for these species derived herein and those tabulated in the ATcT is much improved upon use of the W3X-L method. Using this approach leads to differences in the 0.5–2.0 kJ mol^{-1} range, whereas disagreement had previously been much higher (4.1–7.9 kJ mol^{-1}).

It is interesting to note the difference in enthalpy of formation values for NCN within two consecutive iterations of the ATcT. Comparisons shown in this work are with the latest version (ver. 1.118), in which $\Delta_f H°(298.15\ K) = 456.4$ kJ mol^{-1} for NCN (compared to 454.5 kJ mol^{-1} calculated herein upon utilisation of W3X-L). This contrasts with the 2013 version of ATcT (ver. 1.112) which lists a value of 445.7 kJ mol^{-1}, which is, interestingly, in better agreement with the CBS-APNO/G3/G4 derived value of 448.5 kJ mol^{-1}. This represents a change of 10.7 kJ mol^{-1} between versions, which is well outside of the stated 95% confidence limit of ±1.8 kJ mol^{-1}.[46]

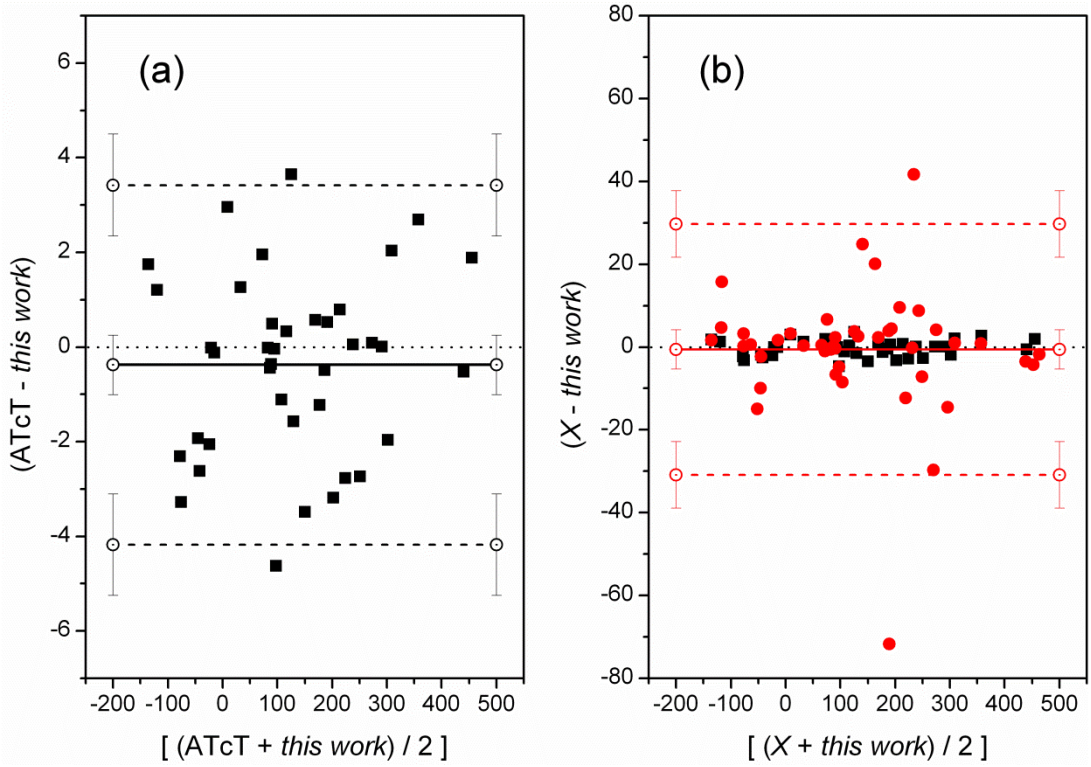

Figure 1. Difference between literature 298.15 K enthalpies of formation and those derived in this study versus the average of the respective values. ■ Black symbols and lines refer to comparisons with ATcT[37], while ● red corresponds to values from Mathieu and Petersen.[16] Solid lines: bias. Dashed lines: 95% limits of agreement. All values are in units of kJ mol^{-1}. Note the difference in y-axis scale.

Figure 1 (b) illustrates the disparity seen amongst values used in literature models, and those presented herein. A literature model, which has been extensively validated against oxidation experiments of CH_4/NO_2, CH_4/N_2O, and NH_3, is used in this particular comparison.[16] Similar levels of agreement are seen when comparing our values against those used in several other recent literature models, which have been validated against experiments designed to aid the elucidation of important thermochemical kinetic parameters (as well as the underlying chemical mechanisms) relevant to NO_x formation. The bias in Fig. 1 (b) is approximately equal to that in Fig. 1 (a), though perhaps fortuitously so. However, the 95% confidence intervals have ballooned to 30.3 kJ mol^{-1}. The difference in scale required in order to plot these results when compared to that required for comparisons with the ATcT illustrates that thermochemical values currently in use in literature models are significantly deficient. Similar plots to those shown in Fig. 1 for other literature models are provided as Supporting Information, as well as comparisons of 298.15 K entropies, in which similar disparities are noted. A detailed analysis of the differences between values in literature models and those presented herein would be most valuable. However, the manuscripts describing the development of these models often make no mention of the source of the thermodynamic data, instead focussing more so on the mechanistic and kinetic aspects of the work.

It would be perhaps unfair to detail each outlier in Fig. 1 (b), as most of the investigated models show similar levels of disagreement with the values determined herein. However, it is worth discussing the one major outlier due to its ubiquity in literature models. Thermochemical values for the hydrazine radical (N_2H_3) are identical in several literature models (including that of Mathieu and Petersen[16]), with a 298.15 K enthalpy of formation equal to 153.9 kJ mol^{-1}. This is compared to a value of 225.6 kJ mol^{-1} derived in this study, which coincidentally is in exceptional agreement with that used in the model of Konnov[11] (225.1 kJ mol^{-1}). A check for internal thermochemical consistency within the models by comparison with hydrazine also reveals this as an erroneous value. As an example, the 298.15 K enthalpy of formation for hydrazine within the Mathieu and Petersen

model[16] is 95.4 kJ mol^{-1}, resulting in a dissociation energy for the $H_2N(H)N–H$ bond of 276.5 kJ mol^{-1} (when the ATcT value of 218.0 kJ mol^{-1} is assumed for atomic hydrogen). This seems an unusually low value for this type of bond, and if a similar analysis is conducted with the values derived in this study, a value of 343.4 kJ mol^{-1} results. This is a more realistic value and compares more favourably with the 347.4 kJ mol^{-1} value calculated when all values used are from the ATcT. Though agreement is within 4 kJ mol^{-1}, closer agreement may be expected given that the comparison is of relative energies, and an interesting point arises. There is a 4.7 kJ mol^{-1} difference between the 298.15 K enthalpy of formation for hydrazine presented in this study (the 0 K value of which is adopted from Simmie[31]) and that in the ATcT. This peculiarity has been highlighted previously (and extensively discussed) by Simmie, with evidence pointing to the ATcT value being uncharacteristically incorrect in this instance. Unusual disparities were noted in the case of hydrazine, in terms of previous experimental and theoretical determinations. A value was reached by Simmie which rationalises trends observed in a series of isodesmic reactions involving methylated hydrazines, the values of which are anchored on that of hydrazine. Internal cross-checks, such as that just described, can prove useful in identification of suspect thermochemical parameters.

3.2. Implications for combustion modelling

The model of Mathieu and Petersen[16] has been used to examine the effects of inclusion of the newly calculated thermochemistry on predictions of nitrogen-containing species under typical gas turbine conditions. Simulations were run using the perfectly-stirred reactor module within CHEMKIN-PRO[40] at a constant pressure of 20 bar, and over a series of residence times up to 20 ms. Inlet conditions were selected to be 720 K, for a mixture comprising 4.87% CH_4, 19.98% O_2, and 75.15% N_2, resulting in an outlet temperature of 1800 K at 20 ms. The simulation results obtained using the original model of Mathieu and Petersen, and those incorporating the updated thermochemical parameters, are plotted in Fig. 2. The three nitrogen-containing species with the highest concentrations at 20 ms residence time are plotted [nitric oxide (NO), nitrogen dioxide (NO_2), and

nitrous oxide (N_2O)], alongside the isomeric pair, nitrous acid (HONO, *trans*- conformer in Fig. 2) and nitryl hydride or isonitrous acid (HNO_2). Nitrogen dioxide mole fractions have been multiplied by 50 in Fig. 2 for illustrative purposes.

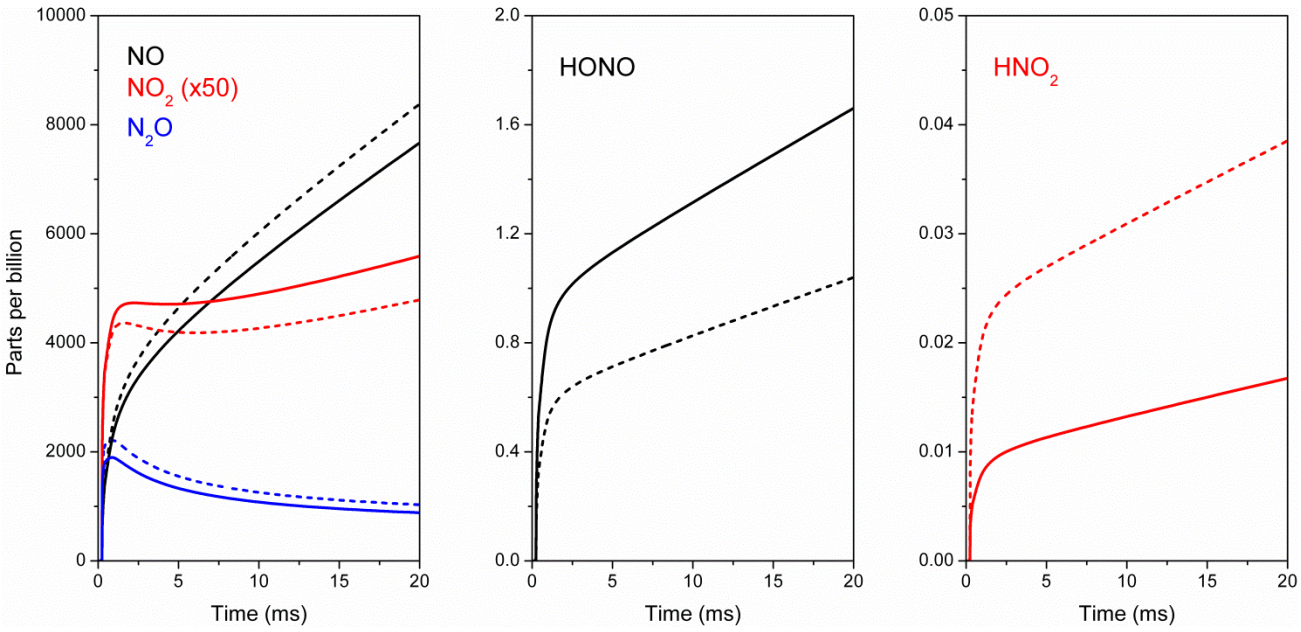

Figure 2. Effects of updating thermochemical values within a literature model[16] on the prediction of several important nitrogenous compounds under typical gas turbine operating conditions. Dashed lines refer to results using the original model, while solid lines correspond to the updated model.

It is shown that there is a decrease of approximately 10 and 20% in NO and N_2O, respectively, at 20 ms residence time upon adoption of the newly calculated thermochemical values, while an increase of ~20% is observed for NO_2 under the sample conditions investigated. While these differences are small, it may be the case that the effect is amplified under other conditions. The relative changes observed in some important NO_x-forming intermediates are not so trivial. HONO and HNO_2 have previously been highlighted as being important sources of hydroxyl radicals and NO_x species under atmospheric and combustion conditions[47,48], and coexist on a PES where final products are sensitive to the thermochemical properties of the species therein.[49] Some striking differences are seen in model-simulated profiles for these isomers in Fig. 2. These results may be

rationalised based on the differences in thermochemical properties of HONO and HNO_2 (which can interconvert between one another) in the original and updated models.

Enthalpy values calculated herein for *trans*-HONO are very similar to those used in the model of Mathieu and Petersen[16]; this study, $\Delta_f H°(298.15\ K) = -76.86$ kJ mol^{-1}, versus –76.73 kJ mol^{-1} used in the Mathieu and Petersen model. Far less agreement is observed between entropies, with our own computations resulting in $S°(298.15\ K) = 256.44$ J K^{-1} mol^{-1}, and a corresponding value of 249.32 J K^{-1} mol^{-1} in the selected literature model. This large entropic difference in *trans*-HONO is coupled with a large enthalpic difference in HNO_2 to produce widely disparate equilibrium coefficients for the isomerisation reaction between the two compounds. In the case of HNO_2, 298.15 K enthalpy of formation values differ by ~14.9 kJ mol^{-1} [–44.27 kJ mol^{-1} (*this study*) versus –59.20 kJ mol^{-1} (Ref. 16)], while entropy values at the same temperature differ only marginally [238.11 J K^{-1} mol^{-1} (*this study*) versus 237.40 J K^{-1} mol^{-1} (Ref. 16)]. This culminates in Gibb's energies of reaction ($\Delta G°_{rxn}$) for the HONO–HNO_2 isomerisation varying by ~17 kJ mol^{-1} at 298.15 K in favour of HONO over HNO_2.

In most detailed chemical kinetic models describing atmospheric and combustion processes, rate coefficients are defined for a reaction in one direction, with the reverse coefficient determined *via* microscopic reversibility. For a given rate coefficient in the forward direction, the magnitude of difference in $\Delta G°_{rxn}$ seen herein for the HONO–HNO_2 isomerisation reaction results in a difference in the rate coefficient in the reverse direction of over a factor of 900 at 298.15 K! This example illustrates the importance of the use of accurate thermochemical values in kinetic models, but these findings may also have ramifications for experimental studies. It is seen that there are relatively small differences in simulated concentrations of NO, NO_2, and N_2O, but that there are significantly larger differences seen in the profiles of species which contribute to their formation. Experimental observation of important intermediates can help to constrain model parameters, and avoid a situation

where a model can predict some of the more major validation targets through a series of compensating erroneous thermochemical kinetic values.

The results of Fig. 2 only apply to these sample conditions, and it may well be that more significant differences exist under other conditions, though these results may be an indication of modelling implications. The major interesting effect observed here is the divergence of relative concentrations. This has ramifications for practical use of chemical kinetic models, as not only are the predicted concentrations quantitatively different, but (often more importantly from a practical standpoint) qualitatively different. This further stresses the importance of having a sound thermochemical base from which further kinetic investigations may begin, with the eventual outcome being a truly predictive model.

4. CONCLUSIONS

This study presents a database of quantum-chemically derived thermochemical functions, with their main intention for use being within chemical kinetic models. Comparisons of these values with those currently in use in literature models show some alarming disagreements, though when they are incorporated into one of these models the simulations results are less so.

An accurate and consistent set of thermochemical parameters is essential within a model, not only in terms of simulation results, but also in order to ensure numerical stability. This is especially important for more computationally demanding simulations, such as 1-D flame speed simulations, where failures are commonplace. It is endemic amongst current literature detailed chemical kinetic models that a reasonable estimate (or indeed a highly accurate value) is employed for a rate coefficient for a reaction in the forward direction, only to be thwarted by an unphysical counterpart in the reverse due to erroneous thermochemistry.

With a comprehensive set of accurate thermochemical values for NO_x-related nitrogen-containing species now available, a review or corresponding update of kinetic rate parameters is needed for the full benefit of our work to be realised.

ACKNOWLEDGEMENTS

The authors wish to acknowledge the support of the Irish Research Council and GE Power Ltd. in funding this project under grant number EPSPG/2012/380. We also acknowledge the provision of computational resources from the Irish Centre for High-End Computing, ICHEC, under project number ngche026c.

SUPPORTING INFORMATION

Literature comparisons, DFT and composite methods output information, tabulated thermochemical data in THERM format, and thermochemical data in NASA polynomials are available as Supporting Information.

REFERENCES

(1) Dagaut, P.; Nicolle, A. Experimental and kinetic modeling study of the effect of SO_2 on the reduction of NO by ammonia. *Proc. Combust. Inst.* **2005,** *30*, 1211–1218.

(2) El Bakali, A.; Pillier, L.; Desgroux, P.; Lefort, B.; Gasnot, L.; Pauwels, J. F.; da Costa, I. NO prediction in natural gas flames using GDF-Kin®3.0 mechanism NCN and HCN contribution to prompt-NO formation. *Fuel* **2006,** *85,* 896–909.

(3) Moréac, G.; Dagaut, P.; Roesler, J. F.; Cathonnet, M. Nitric oxide interactions with hydrocarbon oxidation in a jet-stirred reactor at 10 atm. *Combust. Flame* **2006,** *145,* 512–520.

(4) Dubreuil, A.; Foucher, F.; Mounaïm-Rousselle, C.; Dayma, G.; Dagaut, P. HCCI combustion: Effect of NO in EGR. *Proc. Combust. Inst.* **2007,** *31,* 2879–2886.

(5) Sivaramakrishnan, R.; Brezinsky, K.; Dayma, G.; Dagaut, P. High pressure effects on the mutual sensitization of the oxidation of NO and CH_4–C_2H_6 blends. *Phys. Chem. Chem. Phys.* **2007,** *9,* 4230–4244.

(6) Dagaut, P.; Glarborg, P.; Alzueta, M. U. The oxidation of hydrogen cyanide and related chemistry. *Prog. Energy Combust. Sci.* **2008,** *34,* 1–46.

(7) Rasmussen, C. L.; Hansen, J.; Marshall, P.; Glarborg, P. Experimental measurements and kinetic modeling of $CO/H_2/O_2/NO_x$ conversion at high pressure. *Int. J. Chem. Kinet.* **2008,** *40,* 454–480.

(8) Mével, R.; Javoy, S.; Lafosse, F.; Chaumeix, N.; Dupré, G.; Paillard, C. -E. Hydrogen–nitrous oxide delay times: Shock tube experimental study and kinetic modelling. *Proc. Combust. Inst.* **2009,** *32,* 359–366.

(9) Tian, Z.; Li, Y.; Zhang, L.; Glarborg, P.; Qi, F. An experimental and kinetic modeling study of premixed $NH_3/CH_4/O_2$/Ar flames at low pressure. *Combust. Flame* **2009,** *156,* 1413–1426.

(10) Mendiara, T.; Glarborg, P. Ammonia chemistry in oxy-fuel combustion of methane. *Combust. Flame* **2009,** *156,* 1937–1949.

(11) Konnov, A. A. Implementation of the NCN pathway of prompt-NO formation in the detailed reaction mechanism. *Combust. Flame* **2009,** *156,* 2093–2105.

(12) Giménez-López, J.; Alzueta, M. U.; Rasmussen, C. T.; Marshall, P.; Glarborg, P. High pressure oxidation of C_2H_4/NO mixtures. *Proc. Combust. Inst.* **2001,** *33,* 449–457.

(13) Klippenstein, S. J.; Harding, L. B.; Glarborg, P.; Miller, J. A. The role of NNH in NO formation and control. *Combust. Flame* **2011,** *158,* 774–789.

(14) Duynslaegher, C.; Contino, F.; Vandooren, J.; Jeanmart, H. Modeling of ammonia combustion at low pressure. *Combust. Flame* **2012,** *159,* 2799–2805.

(15) Gokulakrishnan, P.; Fuller, C. C.; Klassen, M. S.; Joklik, R. G.; Kochar, Y. N.; Vaden, S. N.; Lieuwen, T. C.; Seitzman, J. M. Experiments and modeling of propane combustion with vitiation. *Combust. Flame* **2014,** *161,* 2038–2053.

(16) Mathieu, O.; Petersen, E. L. Experimental and modeling study on the high-temperature oxidation of Ammonia and related NOx chemistry. *Combust. Flame* **2015,** *162,* 554–570.

(17) Bohon, M. D.; Al Rashidi, M. J.; Sarathy, S. M.; Roberts, W. L. Experiments and simulations of NO_x formation in the combustion of hydroxylated fuels. *Combust. Flame* **2015,** *162,* 2322–2336.

(18) Mathieu, O.; Pemelton, J. M.; Bourque, G.; Petersen, E. L. Shock-induced ignition of methane sensitized by NO_2 and N_2O. *Combust. Flame* **2015,** *162,* 3053–3070.

(19) Bugler, J.; Somers, K. P.; Silke, E. J.; Curran, H. J. Revisiting the Kinetics and Thermodynamics of the Low-Temperature Oxidation Pathways of Alkanes: A Case Study of the Three Pentane Isomers. *J. Phys. Chem. A* **2015,** *119,* 7510–7527.

(20) Simmie, J. M. Detailed chemical kinetic models for the combustion of hydrocarbon fuels. *Prog. Energy Combust. Sci.* **2003,** *29,* 599–634.

(21) Frenklach, M. Transforming data into knowledge–Process Informatics for combustion chemistry. *Proc. Combust. Inst.* **2007,** *31,* 125–140.

(22) Wang, H.; Sheen, D. A. Combustion kinetic model uncertainty quantification, propagation and minimization. *Prog. Energy Combust. Sci.* **2015,** *47,* 1–31.

(23) Lee, C.; Yang, W.; Parr, R. G. Development of the Colle-Salvetti correlation-energy formula into a functional of the electron density. *Phys. Rev. B* **1988,** *37,* 785–789.

(24) Dunning, T. H. Gaussian basis sets for use in correlated molecular calculations. I. The atoms boron through neon and hydrogen. *J. Chem. Phys.* **1989,** *90,* 1007–1023.

(25) Alecu, I. M.; Zheng, J.; Zhao, Y.; Truhlar, D. G. Computational thermochemistry: Scale factor databases and scale factors for vibrational frequencies obtained from electronic model chemistries. *J. Chem. Theory Comput.* **2010,** *6,* 2872–2887.

(26) Li, X.; Jasper, A. W.; Zádor, J.; Miller, J. A.; Klippenstein, S. J. Theoretical kinetics of O + C_2H_4. *Proc. Combust. Inst.* **2016,** doi:10.1016/j.proci.2016.06.053

(27) Frisch, M. J.; Trucks, G. W.; Schlegel, H. B.; Scuseria, G. E.; Robb, M. A.; Cheeseman, J. R.; Scalmani, G.; Barone, V.; Mennucci, B.; Petersson, G. A.; et al. Gaussian 09, revision D.01, Gaussian, Inc., Wallingford, CT, **2009**.

(28) MultiWell-2014.1 Software, **2014**, designed and maintained by Barker, J. R. with contributors Ortiz, N. F.; Preses, J. M.; Lohr, L. L.; Maranzana, A.; Stimac, P. J.; Nguyen, T. L.; Kumar, T. J. D. University of Michigan, Ann Arbor, MI, http://aoss.engin.umich.edu/multiwell/.

(29) Barone, V. Anharmonic vibrational properties by a fully automated second-order perturbative approach. *J. Chem. Phys.* **2005,** *122,* 014108.

(30) Feller, D.; Peterson, K. A.; Dixon, D. A.; A survey of factors contributing to accurate theoretical predictions of atomization energies and molecular structures. *J. Chem. Phys.* **2008,** *129,* 204105.

(31) Simmie, J. M. A Database of Formation Enthalpies of Nitrogen Species by Compound Methods (CBS-QB3, CBS-APNO, G3, G4). *J. Phys. Chem. A* **2015,** *119,* 10511–10526.

(32) Ochterski, J. W.; Petersson, G. A.; Montgomery, J. A. A complete basis set model chemistry. V. Extensions to six or more heavy atoms. *J. Chem. Phys.* **1996,** *104,* 2598–2619.

(33) Curtiss, L. A.; Raghavachari, K.; Redfern, P. C.; Rassolov, V.; Pople, J. A. Gaussian-3 (G3) theory for molecules containing first and second-row atoms. *J. Chem. Phys.* **1998,** *109,* 7764–7776.

(34) Curtiss, L. A.; Redfern, P. C.; Raghavachari, K. Gaussian-4 theory. *J. Chem. Phys.* **2007,** *126,* 084108.

(35) Simmie, J. M.; Somers, K. P. Benchmarking Compound Methods (CBS-QB3, CBS-APNO, G3, G4, W1BD) against the Active Thermochemical Tables: A Litmus Test for Cost-Effective Molecular Formation Enthalpies. *J. Phys. Chem. A* **2015,** *119,* 7235–7246.

(36) Somers, K. P.; Simmie, J. M. Benchmarking Compound Methods (CBS-QB3, CBS-APNO, G3, G4, W1BD) against the Active Thermochemical Tables: Formation Enthalpies of Radicals. *J. Phys. Chem. A* **2015,** *119,* 8922–8933.

(37) Ruscic, B. Active Thermochemical Tables (ATcT) values based on ver. 1.118 of the Thermochemical Network, **2015,** available at <http://atct.anl.gov/>.

(38) NIST Computational Chemistry Comparison and Benchmark Database, NIST Standard Reference Database Number 101, Release 17b, September **2015,** Editor: Johnson III, R. D. available at <http://cccbdb.nist.gov/>.

(39) Gordon, S.; McBride, B. J. Computer Program for Calculation of Complex Chemical Equilibrium Compositions, Rocket Performance, Incident and Reflected Shocks and Chapman Jouguet Detonations, NASA Report SP-273, **1971**.

(40) CHEMKIN-PRO 15101; Reaction Design: San Diego, **2010**.

(41) Ritter, E. R.; Bozzelli, J. W. THERM: Thermodynamic property estimation for gas phase radicals and molecules. *Int. J. Chem. Kin.* **1991,** *23,* 767–778.

(42) Bland, J. M.; Altman, D. G. Measuring agreement in method comparison studies. *Stat. Methods Med. Res.* **1999,** *8,* 135–160.

(43) Simmie, J. M.; Sheahan, J. A Statistical Overview of a Database of Formation Enthalpies, in preparation.

(44) Chan, B.; Radom L. W2X and W3X-L: Cost-Effective Approximations to W2 and W4 with kJ mol^{-1} Accuracy. *J. Chem. Theory Comput.* **2015,** *11,* 2109–2119.

(45) Lee, T. J.; Taylor, P. R. A Diagnostic for Determining the Quality of Single-Reference Electron Correlation Methods. *Int. J. Quantum Chem. Quantum Chem. Symp.* **1989,** *23,* 199–207.

(46) Ruscic, B. Active Thermochemical Tables (ATcT) values based on ver. 1.112 of the Thermochemical Network, **2013,** available at <http://atct.anl.gov/>.

(47) Nguyen, M. T.; Sumathi, R.; Sengupta, D.; Peeters, J. Theoretical analysis of reactions related to the HNO_2 energy surface: OH + NO and H + NO_2. *Chem. Phys.* **1998,** *230,* 1–11.

(48) Asatryan, R.; Bozzelli, J. W.; Simmie, J. M. Thermochemistry for Enthalpies and Reaction Paths of Nitrous Acid Isomers. *Int. J. Chem. Kinet.* **2007,** *39,* 378–398.

(49) Miller, J. A.; Melius, C. F. The reactions of imidogen with nitric oxide and molecular oxygen. *Symp. Int. Combust. Proc.* **1992,** *24,* 719–726.